Current Research in Food Science 8 (2024) 100756

Contents lists available at ScienceDirect

Current Research in Food Science

journal homepage: www.sciencedirect.com/journal/current-research-in-food-science

Efficient biosynthesis of transglutaminase in *Streptomyces mobaraensis* via systematic engineering strategies

Fang Yuan [a], Guoying Li [b], Zilong Li [c], Mingming Li [b], Xiaobo Liu [d,*], Haiquan Yang [a,**], Xiaobin Yu [a,***]

[a] *The Key Laboratory of Industrial Biotechnology, Ministry of Education, School of Biotechnology, Jiangnan University, Wuxi, 214122, China*
[b] *Jiangsu Yiming Biological Technology Co., Ltd., Taixing, 225400, China*
[c] *State Key Laboratory of Microbial Resources, Institute of Microbiology, Chinese Academy of Sciences, Beijing, 100101, China*
[d] *Key Laboratory of Metabolic Engineering and Biosynthesis Technology, Ministry of Industry and Information Technology, Nanjing University of Science and Technology, 200 Xiaolingwei Street, Nanjing, Jiangsu, 210094, China*

ARTICLE INFO

Handling Editor: Dr. Quancai Sun

Keywords:
Transglutaminases
Industrial production
Signal peptide
Promoter
Multiple copies
Recombination sites

ABSTRACT

Transglutaminases (TGases) have been widely used in food, pharmaceutical, biotechnology, and other industries because of their ability to catalyze deamidation, acyl transfer, and crosslinking reactions between γ-carboxamide groups of peptides or protein-bound glutamine and the ε-amino group of lysine. In this study, we demonstrated an efficient systematic engineering strategy to enhance the synthesis of TGase in a recombinant *Streptomyces mobaraensis* smL2020 strain in a 1000-L fermentor. Briefly, the enzymatic properties of the TGase TG_{L2020} from *S. mobaraensis* smL2020 and TGase TG_{LD} from *S. mobaraensis* smLD were compared to obtain the TGase TG_{LD} with perfected characteristics for heterologous expression in a recombinant *S. mobaraensis* smL2020ΔTG without the gene $tg_{L\ 2020}$. Through multiple engineering strategies, including promoter engineering, optimizing the signal peptides and recombination sites, and increasing copies of the expression cassettes, the final TG_{LD} activity in the recombinant *S. mobaraensis* smL2020ΔTG: $(P_{L2020}\text{-}sp_{L2020}\text{-}protg_{LD}\text{-}tg_{LD})_2$ (tg_{L2020} *and* BT1) reached 56.43 U/mL and 63.18 U/mL in shake flask and 1000-L fermentor, respectively, which was the highest reported to date. With the improvement of expression level, the application scope of TG_{LD} in the food industry will continue to expand. Moreover, the genetic stability of the recombinant strain maintained at more than 20 generations. These findings proved the feasibility of multiple systematic engineering strategies in synthetic biology and provided an emerging solution to improve biosynthesis of industrial enzymes.

1. Introduction

Transglutaminase (protein-glutamine γ-glutamyltransferase, TGase, EC 2.3.2.13) can catalyze deamidation, acyl transfer, and crosslinking reactions between a γ-carboxamide group of a peptide or a protein-bound glutamine and ε-amino group of lysine, in which glutamine is the acyl donor and lysine is the acyl acceptor (Jiang et al., 2017; Luisa et al., 2015). TGases have been widely used in food, pharmaceutical, textile, biotechnology, and other industries because of their ability to efficiently covalently modify other proteins (Duarte et al., 2020; Yin et al., 2021). Additionally, the texture properties of different foods (e.g., dairy products and meat products) have been enhanced by TGases (Duarte et al., 2020; Santhi et al., 2017).

The microbial TGases have many advantages compared with TGases from animals and plants, including relatively high activity in a wide range of pH and temperatures, Ca^{2+}-independence, and no special cofactor requirements (Luisa et al., 2015). Although microbial TGases have been obtained from different microorganisms, including *Streptomyces hygroscopicus*, *Streptoverticillium mobaraensis*, *Bacillus subtilis*, and *B. circulans* (Cui et al., 2008; Luís et al., 2003; Zheng et al., 2002), the production of microbial TGases is still challengeable. For example, the intracellular TGases from *B. subtilis* were originally considered as an alternative candidate for catalyzing modification reactions of proteins (Fernandes et al., 2019; Monroe and Setlow, 2006). However, the

* Corresponding author.
** Corresponding author.
*** Corresponding author.
E-mail addresses: xbliu@njust.edu.cn (X. Liu), haiquanyang@jiangnan.edu.cn (H. Yang), xbyu@jiangnan.edu.cn (X. Yu).

https://doi.org/10.1016/j.crfs.2024.100756
Received 22 January 2024; Received in revised form 7 March 2024; Accepted 30 April 2024
Available online 1 May 2024

versatility of TGases from *B. subtilis* was limited and its manufacturing process was difficult (KOBAYASHI et al., 1998). TGases from *S. mobaraensis* are recognized safe by the U.S. Food and Drug Administration (Yin et al., 2021). Thus, microbial TGases used in food industry have been mainly produced in *S. mobaraensis* (Yokoyama et al., 2004). However, TGases from *S. mobaraensis* are expressed as inactive zymogens to avoided uncontrolled cross-linking of cellular proteins and required to be activated by a serine and a metalloprotease, where pro-regions of the zymogens are removed (Zhang et al., 2012). Moreover, the activities of microbial TGases from wild-type strains are very limited. For example, the highest activity of the microbial TGase from *Streptoverticillium* strain S-8112 was only approximately 2.5 U•mL^{-1} (ANDO et al., 1989).

Different fermentation optimization and microbial breeding strategies have been used to improve production of microbial TGases in *S. mobaraensis*, such as non-nutritional stress, two-stage fermentation strategies, supplementing with excessive $MgCl_2$, and atmospheric and room-temperature plasma (ARTP) mutagenesis (Bagagli and Sato, 2013; Jiang et al., 2017; Yin et al., 2021). Zhang et al. (2012) studied the effects of eight different salts for stress-mediated bioprocesses of the production of TGase in *S. mobaraensis*, and it was found that the highest TGase activity (4.3 U•mL^{-1}) was obtained by supplementing 100 mM $MgCl_2$. ARTP mutagenesis and site-directed genetic modifications were used to improve the TGase activity of *S. mobaraensis*, and TGase activity in *S. mobaraensis* smY 2019-3C reached 40 U/mL (Yin et al., 2021). However, these simple strategies have their limitation in improving the activities or productivities of TGases, and thus further studies on systematic engineering strategies are needed to be developed.

In this study, we used systematic engineering strategies to construct a recombinant *S. mobaraensis* strain with high industrial productivity of the TGase TG_{LD} with perfected characteristics in a 1000-L fermentor. In detail, the enzymatic properties of the TGase TG_{L2020} from *S. mobaraensis* smL2020 and the TGase TG_{LD} from *S. mobaraensis* smLD were compared, and the TGase TG_{LD} with perfected characteristics was chosen to enhance the TGase production level. Signal peptide optimization and promoter engineering were used to improve the heterologous expression level of tg_{LD} in *S. mobaraensis* smL2020ΔTG. Copies and recombination sites of the tg_{LD} gene expression cassette were optimized to improve its heterologous expression level in *S. mobaraensis* smL2020ΔTG. The TGase TG_{LD} in *S. mobaraensis* smL2020ΔTG: (P_{L2020}-sp_{L2020}-$protg_{LD}$-tg_{LD})$_2$ (tg_{L2020} and BT1) was produced in a 1000-L fermentor.

2. Materials and methods

2.1. Strains and plasmids

S. mobaraensis smL2020(CGMCC29945) and *E. coli* DH5α were stored in our lab (Fermentation and Health food Laboratory, School of Biotechnology, Jiangnan University, China). *S. mobaraensis* smLD (CGMCC4.1851) was obtained from the China General Microbiological Culture Collection Center (CGMCC). *E. coli* ET12567/pUZ8002, and plasmids pKC1132, pSET152, and pSET156 were obtained from the Institute of Microbiology, Chinese Academy of Sciences. *E. coli* ET12567/pUZ8002 was the conjugal transfer demethylation donor, including the gene *tra*. Plasmid pKC1132 was a suicide plasmid, without replicons of *Streptomyces*, and with the conjugal transfer site *oriT* and amprimycin resistance gene *acc(3)IV*. Plasmids pSET152 and pSET156 were used for gene integration, which included genes *ΦC31-attP* and *BT1-attP*, respectively (Bierman et al., 1992; Zhengyao et al., 2008). Primers used in the study were shown in Table S1. Plasmid and strains constructed in this study were shown in Tables S2 and S3.

2.2. Instrumentation and reagents

The main instrumentations used in this study were shown in Table S4. O-carboxybenzoyl-L-glutaminyl-glycine (N-CBZ-Gln-Gly) was purchased from Jill Biochemical (Shanghai) Co., Ltd. L-Glutamic acid-γ-monohydroxylamine was purchased from Sigma-Aldrich. Reduced glutathione was purchased from Shanghai Maclean's Biochemical Technology Co., Ltd. Standard molecular weight protein and 12% Tris-glycine SDS-PAGE gels were purchased from Thermo Fisher (Shanghai). Plasmid mini-extraction kit, bacterial genomic DNA extraction kit, DNA glue recovery kit, were purchased from Nanjing Vazyme Biotechnology Co., Ltd. Ampicillin, ampramycin and lysozyme were purchased from Sangon Bioengineering (Shanghai) Co., Ltd. Restriction enzymes, DNA ligases, and DNA polymerases were purchased from TaKaRa (Dalian). Tryptone, malt extract and yeast extract were purchased from Oxoid (UK). The other reagents were all made in China and analytical pure.

2.3. Media and culture conditions

The 2 × YT medium consisted of 16 g/L tryptone, 10 g/L yeast extract, and 5 g/L NaCl. PDA medium consisted of 20 g/L potato, 2 g/L glucose, and 20 g/L agar. LB solid medium consisted of 10 g/L tryptone, 5 g/L yeast extract, 10 g/L NaCl, and 20 g/L agar at pH 7.0. Mannitol soya flour (MS) medium consisted of 20 g/L mannitol, 20 g/L soya flour, and 20 g/L agar, which was used for culturing spores of *S. mobaraensis* and the conjugal transfer. Gauze's synthetic broth medium consisted of 20 g/L glycerol, 20 g/L peptone, 5 g/L yeast extract, 2 g/L $MgSO_4{\cdot}7H_2O$, and 2 g/L $K_2HPO_4{\cdot}3H_2O$ at pH 7.4. The seed medium consisted of 20 g/L glycerol, 20 g/L peptone, 5 g/L yeast extract, 2.5 g/L corn steep liquor, 2.5 g/L $MgSO_4{\cdot}7H_2O$, and 2 g/L $K_2HPO_4{\cdot}3H_2O$ at pH 7.4. The fermentation medium consisted of 20 g/L glycerol, 20 g/L peptone, 5 g/L yeast extract, 5 g/L corn steep liquor, 2 g/L $MgSO_4{\cdot}7H_2O$, 4 g/L $K_2HPO_4{\cdot}3H_2O$, 2 g/L $KH_2PO_4{\cdot}3H_2O$, and 2 g/L $CaCO_3$ at pH 7.4.

Spores of *S. mobaraensis* smL2020 and *S. mobaraensis* smLD were cultured on solid MS medium at 30 °C for 5 d. Spores were collected with sterilized saline solution, and were inoculated in 50 mL of seed medium (250-mL flask) at 30 °C and 200 rpm for 24 h. Then, 10% (v/v) of the seed was inoculated in 50 mL of fermentation medium (250-mL flask) at 30 °C and 200 rpm for 48 h. For the production of TGase in recombinant *S. mobaraensis* in a 1000-L fermentor, the fermentation conditions were: 10% (v/v) seed inoculant, 400 rpm (stirring speed), 1 vvm, and 0.1 MPa. The fermentation liquid was centrifuged at 5000×*g* for 30 min, and the supernatant was used for determining TGase activity and SDS-PAGE analysis.

2.4. Genomic DNA extraction of S. mobaraensis and E. Coli

Appropriate amounts of *S. mobaraensis* smL2020 and smLD spores were inoculated in the seed medium, incubated at 30 °C for 24 h, and then the seed solution was centrifuged at 4000 rpm for 10 min. The mycelium was collected and washed twice with sterile water. After repeated freeze-thaw cycles, the genomic DNA of the processed sample was extracted according to the steps of the bacterial genomic DNA extraction kit, strictly referring to the instructions of the kit. *E. coli* plasmid DNA was extracted using the plasmid mini-extraction kit, and the specific steps were shown in the kit instructions.

2.5. Preparation and transformation of E. Coli competent cells

1 mL of overnight cultured *E. coli* solution was inoculated into 100 mL of LB liquid medium, incubated at 37 °C and 220 rpm shaker for 2–3 h until the OD600 was 0.4–0.6, and then the culture flask was taken out and placed on ice for 10 min to cool. The cells were recovered by transferring the bacterial solution to a sterile, ice-cooled 50 mL polypropylene tube in a clean bench and centrifuging at 4 °C at 4000 rpm for 10 min. Poured out the culture medium and invert the tube for 1 min to allow the last trace of the culture medium to drain out. Each cell precipitate was resuspended with 30 mL of pre-chilled 0.1 M $MgCl_2$–$CaCl_2$ ($MgCl_2$ 80 mM; $CaCl_2$ 20 mM) per 50 mL initial culture medium and then centrifuged at 4000 rpm for 10 min at 4 °C to recover cells. Poured out

the solution and invert the tube for 1 min to allow the last trace of the culture medium to drain out. Resuspend each cell precipitate with 2 mL of pre-chilled 0.1 M $CaCl_2$ solution per 50 mL initial culture medium. The cell fluid was placed on ice for 1–4 h, then aliquoted at 100–150 μL per tube into pre-chilled centrifuge tubes, and the competent cells were frozen with liquid nitrogen and stored in a −80 °C freezer.

Competent cells were taken out of the −80 °C freezer and dissolved on ice (about 5 min). When the last ice of competent cells melted, the ligation reaction product (5 μL) was transferred to 50 μL of competent cells in EP tube. The bottom of the tube was mixed with a few flicks, and placed on ice for 20–30 min. The conversion tube was removed and fixed on the floating plate, and was heat-shocked at 42 °C for 45–90 s. After that, it was placed on ice for 2–10 min, then at room temperature for 2 min. Five hundred μL of antibiotic-free and sterile LB was taken in a clean bench, and the cells were revived by shaking at 37 °C for 60 min, then centrifuged at 4000 rpm for 5 min. The supernatant after centrifugation was poured out to 100–200 μL in a sterile table, and then the cells were resuspended. After that, the resuspended liquid was coated into resistant plates, and incubated at 37 °C for 16 h to observe the colonies.

2.6. Purification of TGase

For the wild-type TGase, the supernatant was collected by centrifugation and concentrated by an ultrafiltration membrane of 10 kDa (molecular weight) four times at 10−15 °C (Lu et al., 2003). Pre-cooled ethanol was added (final concentration = 60%, v/v) and the precipitate was obtained by centrifugation. The precipitate was dissolved with a 20 mM Tris-HCl buffer (pH 8.0), which was centrifuged at 8000×*g* for 10 min to remove the insoluble matter, and then filtered using a 0.22-μm membrane. TGase was purified by an SP70 ion exchange column. The eluent buffer was a 20 mM Tris-HCl buffer (pH 8.0) with 1.0 M NaCl, and TGase was purified by desalting with a Superdex 75 column (GE Healthcare, New York, USA).

For recombinant TGase with a His 6 tag, the supernatant was collected by centrifugation. A His-Trap Ni^{2+} column (GE Healthcare, New York, USA) was used for purification of recombinant TGase, and 20 mM Na_2HPO_4–NaH_2PO_4 buffer (pH 7.4) with 50 mM NaCl and 300 mM imidazole was used for the eluent buffer. TGase was purified by desalting with a Superdex 75 column (GE Healthcare, New York, USA).

2.7. Determination of TGase enzymatic properties

The enzymatic properties of the purified TGase were determined. The optimal temperature of TGase activity was evaluated at 25, 37, 40, 45, 50, 55, and 60 °C. The thermal stability of TGase was evaluated by incubating at 25, 37, 40, 45, 50, 55, and 60 °C for 1 h. The half-life ($t_{1/2}$) was determined at 50, 55, and 60 °C. The optimum pH of TGase was evaluated at pH 3, 4, 5, 6, 7, 8, 9, 11, and 12. The pH stability of TGase was determined by incubating at 25 °C and pH 3, 4, 5, 6, 7, 8, 9, 11, and 12 for 1 h, respectively.

2.8. Determination of the cross-linking protein function of TGase

Sodium caseinate (Tatua, New Zealand) was used as the substrate to determine the cross-linking protein function of TGase (Lorenzen, 2008). Tris-HCl buffer (pH 8.0) was used to prepare a sodium caseinate solution (3 mg/mL). The TGase was added to a final concentration of 0.01 mg/mL at 40 and 50 °C.

2.9. Conjugal transfer of genes between E. Coli and S. mobaraensis smL2020

The method for conjugal transfer was performed according to the manual for *Streptomyces* with slight modifications (Gil et al., 1985). The specific steps were as follows: a) YT medium (2 ×) was used to collect the spores (10^8–10^9) of *S. mobaraensis* smL 2020, which were then incubated at 50 °C for 10 min for pre-germination. The cooled spores were collected by centrifugation and resuspended in 100 μL of 2 × YT medium as the conjugal transfer recipient. b) *E. coli* ET12567 with pUZ8002 (donor) was inoculated in LB medium, and cultivated at 37 °C until an OD_{600} of 0.4–0.6. Cells were collected by centrifugation (Esmaeilnejad-Ahranjani and Hajimoradi, 2022), washed twice with fresh LB medium, and the supernatant was removed. Then, 200 μL of 2 × YT was used to resuspend cells as the conjugal transfer donor. c) A 200-μL E. *coli* donor suspension was mixed with 100 μL of a spore suspension (recipient), which was cultured on MS medium with 10 mM $MgCl_2$ and 30 mM $CaCl_2$. d) Strains were cultured at 30 °C for 8–10 h with 1 mL of sterile water containing 25 μL of nalidixic acid (25 mg/mL) and 25 μL apramycin (50 mg/mL). e) Strains were cultured at 30 °C for 5–6 d. The suspected positive colonies grown on the plate were transferred to MS medium with 25 μg/mL nalidixic acid and 50 μg/mL apramycin.

2.10. Construction of S. mobaraensis smLD with different TGase gene copies

Recombinant plasmids containing 1–3 copies of the TGase genes were constructed (Fig. S1). Gene fragment P_{LD}-sp_{LD}-$protg_{LD}$-tg_{LD}-T_{tgLD} (1800 bp), including the TGase gene tg_{LD} and its flanking regions, was amplified using primers TGLD-FW and TGLD-RS and the genome of *S. mobaraensis* smLD (template). The promoter was P_{LD}, and the terminator was T_{tgLD}. Plasmid pSET152-*1*tg_{LD} was constructed by linking the obtained gene fragment P_{LD}-sp_{LD}-$protg_{LD}$-tg_{LD}-T_{tgLD} and the pSET152 vector linearized by *BamH* I through homologous recombination. Recombinant plasmid pSET152-*2*tg_{LD} was constructed by linking pSET152-*1tg* and P_{LD}-sp_{LD}-$protg_{LD}$-tg_{LD}-T_{tgLD} using restriction endonucleases *Bgl* II and *Xba* I. Using the same method, recombinant plasmid pSET152-*3*tg_{LD} was constructed based on pSET152-*2*tg_{LD}. Plasmids pSET152-*1*tg_{LD}, pSET152-*2*tg_{LD} and pSET152-*3*tg_{LD} were transformed into *E. coli* ET12567 (pUZ8002), which were conjugatively transferred with *S. mobaraensis* smLD to obtain the recombinant strains *S. mobaraensis* 152-smLD-1C, *S. mobaraensis* 152-smLD-2C, and *S. mobaraensis* 152-smLD-3C with two expression cassettes of P_{LD}-sp_{LD}-$protg_{LD}$-tg_{LD}-T_{tgLD} (pSET152-*1*tg_{LD}), three expression cassettes of P_{LD}-sp_{LD}-$protg_{LD}$-tg_{LD}-T_{tgLD} (pSET152-*2*tg_{LD}) and four expression cassettes of P_{LD}-sp_{LD}-$protg_{LD}$-tg_{LD}-T_{tgLD} (pSET152-*3*tg_{LD}), respectively.

2.11. Construction of S. mobaraensis smL2020ΔTG without the TGase gene

Using pKC1132 as the starting plasmid, the gene *gfp* was linked with plasmid pKC1132 to obtain the recombinant plasmid pKC1132-*gfp* (Urban and Vogel, 2009). The upstream and downstream homology arms (3000 bp) of gene tg_{L2020} were amplified by primers TG-up-FW and TG-up-RS, and with TG-down-FW and TG-down-RS, respectively, using *S. mobaraensis* smL2020 DNA as a template. Plasmid pKC1132-*gfp* was linked with the upstream and downstream homology arms using Gibson assembly technology to construct the recombinant knockout plasmid pKC1132-*gfp*-dtg_{L2020}. Plasmid pKC1132-*gfp*-dtg_{L2020} was transformed into *E. coli* ET12567 (pUZ8002), which was conjugatively transferred with *S. mobaraensis* smL2020 to construct *S. mobaraensis* smL2020ΔTG with the knockout gene $tg_{L\ 2020}$. Because pKC1132-*gfp*-dtg_{L2020} was a suicide plasmid, it did not have *Streptomyces* replicons and could not survive in the host, but the gene fragments 3000 bp upstream and downstream of the TG_{L2020} gene carried by pKC1132-*gfp*-dtg_{L2020} were identical to those on the genome of *S. mobaraensis* smL 2020. Plasmid pKC1132-*gfp*-dtg_{L2020} was inserted into the chromosome by a single crossover. After the single crossover process, the positive colonies not only expressed green fluorescent protein (GFP) but also grew on the solid MS medium with apramycin. Screened colonies were transferred to the non-resistant MS medium to further screen for double crossover

colonies. Positive colonies were verified by PCR using primers dTG-test-FW and dTG-test-RS.

2.12. Effects of different signal peptides and promoters on the production of TG_{LD} in S. mobaraensis smL2020ΔTG

The signal peptide SP_{L2020} of TGase in *S. mobaraensis* smL2020 was amplified using the *S. mobaraensis* smL2020 genome as a template by primers SPL2020-FW and SPL2020-RS. The signal peptide SP_{PI} of the papain inhibitor was amplified using the *S. mobaraensis* smLD genome as a template by primers SPmu-FW and SPmu-RS. The signal peptide SP_{SI} of a subtilase-type protease inhibitor was amplified using the *S. mobaraensis* smLD genome as a template by primers SPsti-FW and SPsti-RS. Signal peptides $SP_{L\ 2020}$, SP_{PI}, and SP_{SI} were integrated into the plasmid pSET152-*1*tg_{LD} by restriction enzyme digestion and homologous recombination, to replace the original signal peptide SP_{LD} in pSET152-*1*tg_{LD}, respectively. The recombinant plasmids were named pSET152-sp_{L2020}-tg_{LD}, pSET152-sp_{PI}-tg_{LD}, and pSET152-sp_{SI}-tg_{LD}, respectively.

A promoter mutant sequence P_{mLD} with a G→A mutation in the −10 region and gene tg_{LD} were amplified using the *S. mobaraensis* smLD genome as a template by primers TGLD-FW and TGmLD-R and by primers TGmLD-FW and TGLD-RS (Zhou et al., 2019). P_{mLD} and the gene tg_{LD} were linked with the plasmid pSET152 linearized by *Bam*H I to construct recombinant pSET152-P_{mLD}-tg_{LD}. The promoter sequence fragment $P_{L\ 2020}$ (520 bp) of the gene tg_{L2020} upstream from *S. mobaraensis* smL2020 was amplified using the *S. mobaraensis* smL2020 genome as a template by primers PtgL2020-FW and PtgL2020-RS. The upstream promoter sequence and signal peptide sequence fragment P_{L2020}+$sp_{L\ 2020}$ (600 bp) was amplified using the *S. mobaraensis* smL2020 genome as a template by primers PtgL2020-FW and SPL2020-RS. The upstream promoter sequence, signal peptide sequence, and precursor pro-region fragment P_{L2020}+sp_{L2020}+*ProL 2020* (750 bp) was amplified using the *S. mobaraensis* smL2020 genome as a template by primers PtgL2020-FW and ProL2020-RS. The above three gene fragments were connected with the gene fragment tg_{LD} to obtain three different TGase expression cassettes, which were named C1, C2, and C3. C1, C2, and C3 were linked with plasmid pSET152 linearized by *Bam*H I to construct recombinant pSET152-tg_{LD}*C1*, pSET152-tg_{LD}*C2*, and pSET152-tg_{LD}*C3*, respectively. These plasmids were transformed into *E. coli* ET12567 (pUZ8002), which was conjugatively transferred with *S. mobaraensis* smL2020ΔTG to construct different recombinant *S. mobaraensis* smL2020ΔTG strains.

2.13. Construction of the S. mobaraensis smL2020ΔTG over-expressing gene tg_{LD} from S. mobaraensis smLD

Based on the multi-copy expression of site-specific recombination, plasmids pSET152 containing 1, 2, or 3 copies of the tg_{LD} expression cassette P_{LD}-sp_{LD}-$protg_{LD}$-tg_{LD} from *S. mobaraensis* smLD were transformed into *S. mobaraensis* smL2020ΔTG to construct *S. mobaraensis* smL2020ΔTG::P_{LD}-sp_{LD}-$protg_{LD}$-tg_{LD}, *S. mobaraensis* smL2020ΔTG: (P_{LD}-sp_{LD}-$protg_{LD}$-tg_{LD})$_2$, and *S. mobaraensis* smL2020ΔTG: (P_{LD}-sp_{LD}-$protg_{LD}$-tg_{LD})$_3$, respectively.

2.14. Construction of recombinant S. mobaraensis strains using different recombination sites

The gene fragment tg_{LD} (1800 bp) was amplified using the *S. mobaraensis* smLD genome as a template by primers TGLD-FW and TGLD-RS, and was linked with plasmid pSET156 linearized with *Bam*H I via homologous recombination. The recombinant plasmid pSET156-P_{LD}-tg_{LD} was constructed. Plasmids pSET156-P_{mLD}-tg_{LD} and pSET156-P_{L2020}-tg_{LD} were constructed using the same method. The plasmids were transformed into *E. coli* ET12567 (pUZ8002), which was conjugatively transferred with *S. mobaraensis* smL2020ΔTG to construct different recombinant *S. mobaraensis* smL2020ΔTG strains with tg_{LD} expression cassettes with different promoters at the recombination sites BTI.

Using homologous recombination, the gene tg_{LD} was expressed at the position of the original TGase gene in *S. mobaraensis* smL2020ΔTG. Plasmid pKC1132-*KiTGW* was digested with *Not* I and *EcoR* V for linearization to obtain a gene fragment (6880 bp). The gene fragment P_{LD}-tg_{LD} (1800 bp) was amplified using plasmid pSET152-P_{LD}-tg_{LD} as a template by primers TG_{LD}-FW and TG_{LD}-RS. The gene fragment P_{L2020}-tg_{LD} (1610 bp) was amplified using the plasmid pSET152-P_{L2020}-tg_{LD} as a template by primers copy-FW and copy-RS. The downstream homology arm sequence (2900 bp) was amplified using *S. mobaraensis* smL2020 as a template by primers Ki-FW and Ki-RS. The linearized plasmids and the downstream homology arm sequence were linked via homologous recombination to construct pKC1132-P_{LD}-tg_{LD} and pKC1132-P_{L2020}-tg_{LD}. The plasmids were transformed into *E. coli* ET12567 (pUZ8002), which was conjugatively transferred with *S. mobaraensis* smL2020ΔTG to construct different recombinant *S. mobaraensis* smL2020ΔTG strains with tg_{LD} expression cassettes at the position of the original TGase gene in *S. mobaraensis* smL2020ΔTG.

2.15. Determination of TGase activity

A standard curve was drawn based on L-glutamic acid-γ-monohydroxamic acid. CBZ-Gln-Gly was the substrate used for determining TGase activity (Folk and Cole, 1966). The reaction system included 100 μL of TGase solution, 1000 μL of substrate solution, 30 mM CBZ-Gln-Gly, 100 mM hydroxylamine, 10 mM glutathione, and 200 mM pH 6.0 Tris-HCl buffer. The mixture was incubated at 37 °C for 10 min. Finally, 1000 μL of the terminator, which included 1 M HCl, 4% (v/v) trichloroacetic acid, and 2% (m/v) $FeCl_3$•$6H_2O$, was added to terminate the enzymatic reaction. The absorbance of the reaction solution was measured at 525 nm. One unit (U) of TGase activity was defined as the amount of enzyme catalyzing 1 μmol of substrate per minute to form product.

2.16. Statistical analysis

The means ± standard deviations were obtained from three parallel experiments. Student's t-test was used to statistically analyze data. Statistical significance was set at P value < 0.05.

3. Results and discussion

3.1. Comparison of the enzymatic properties of TGases

Tgase TG_{L2020} from *S. mobaraensis* smL2020 and Tgase TG_{LD} from *S. mobaraensis* smLD were expressed and purified (Fig. S2). Kinetic parameters, optimum pH, pH stability, optimum temperature, thermal stability, and crosslinking of purified TG_{L2020} and TG_{LD} were determined and compared. The assay of kinetic constants is continuous and efficient, allowing rapid comparison between different variants (Kashiwagi et al., 2002). As shown in Table S5, the K_m value of TG_{LD} was 13.45 mM, which was lower than that (18.61 mM) of $TG_{L\ 2020}$ ($P = 0.01$), indicating that the affinity of TG_{LD} to the substrate was higher than that of $TG_{L\ 2020}$. Moreover, the k_{cat} value (18.49 s^{-1}) of TG_{LD} was higher than that (13.82 s^{-1}) of $TG_{L\ 2020}$ ($P = 0.02$) and the k_{cat}/K_m value (1375 L mol^{-1}•s^{-1}) of TG_{LD} was also larger than that (743 L mol^{-1}•s^{-1}) of $TG_{L\ 2020}$ ($P < 0.01$), suggesting that the catalytic efficiency of TG_{LD} was significantly higher than that of $TG_{L\ 2020}$ (Bauer et al., 2001). Compared with the kinetic parameters of the TG enzyme derived from *S. mobaraensis* expressed in *E. coli* by Oteng et al. (Oteng-Pabi and Keillor, 2013), the difference was significant, which may be due to different expression hosts.

The optimum temperature of TG_{L2020} was 45 °C, and the optimum pH of TG_{L2020} was 6.0 (Fig. 1A and B). In contrast, the optimum temperature of TG_{LD} was 50 °C, and optimum pH of TG_{LD} was 7.0. As shown in Fig. 1C, the thermal stability of TG_{LD} was higher than that of $TG_{L\ 2020}$. For example, after incubation at 55 °C for 30 min, the relative residual activity of TG_{LD} was 52% but the relative residual activity of TG_{L2020} was

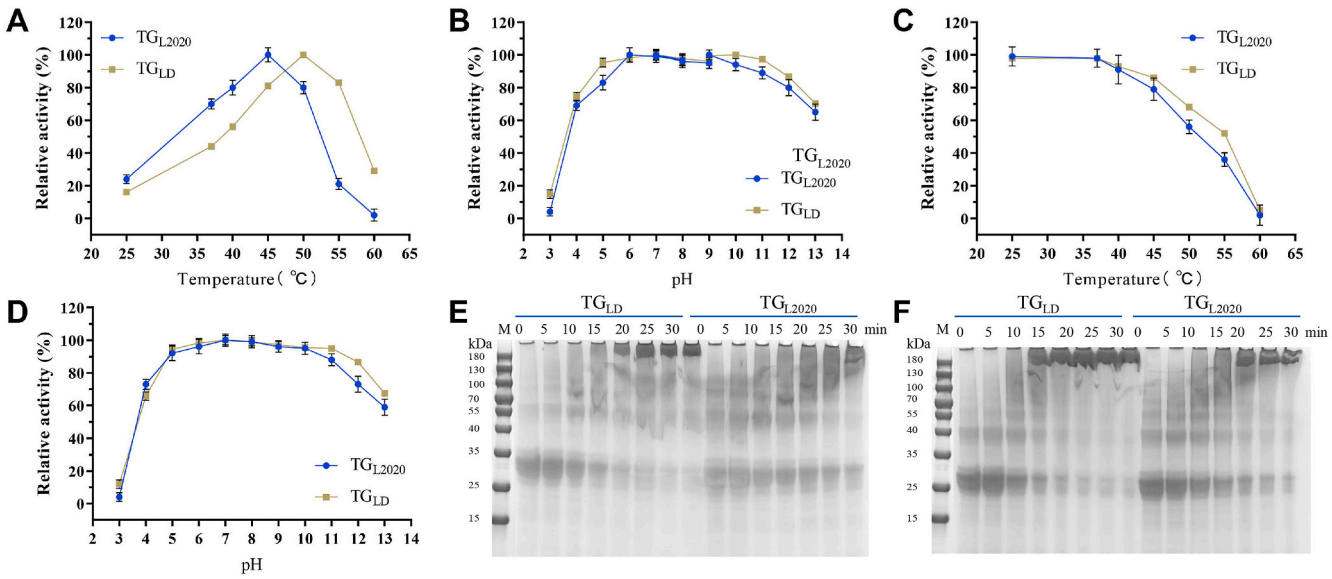

Fig. 1. Comparison of the enzymatic properties of the TGase TG_{L2020} from *S. mobaraensis* smL2020 and the TGase TG_{LD} from *S. mobaraensis* smLD. A, Optimum temperature. B, Optimum pH. C, Thermal stability. D, pH stability. E, Crosslinking of purified TG_{L2020} and TG_{LD} for the β-casein (approximately 28 kDa) at 40 °C. F, Crosslinking of purified TG_{L2020} and TG_{LD} for the β-casein (approximately 28 kDa) at 50 °C. Arrows, Uncrosslinked β-casein bonds. M, Standard weight proteins (Marker).

only 36%. The half-life ($t_{1/2}$) of TG_{LD} was 130 min at 50 °C, which was 3-fold that of $TG_{L\ 2020}$ (Table S5). The $t_{1/2}$ of TG_{LD} was 20 min at 55 °C, which was 1.9-fold that of $TG_{L\ 2020}$. The pH stability of TG_{LD} was also higher than that of $TG_{L\ 2020}$ (Fig. 1D). In industrial practice, TGase preparations were used in powder form, and higher thermal stability means less loss of activity during storage. The pH range of TG_{LD} that retained more than 80% relative residual activity was 5.0–12.0. The pH stability of TG_{LD} was also higher than that of $TG_{L\ 2020}$. The pH range of TG_{LD} with more than 80% relative residual activity was 5.0–11.0. These results indicated that the stability of TG_{LD} was higher than that of $TG_{L\ 2020}$. The optimal temperature and pH of the two purified TGases obtained in this study were similar to the reported TGases of *S. hygroscopicus* and *S. mobaraensis* (ANDO et al., 1989).

β-Casein was used as a substrate to determine the cross-linking effect of TGase produced by the microorganism (Evanthia Monogioudi et al., 2009). In this study, the β-casein band (approximately 28 kDa) became thinner gradually after incubation of TG_{LD} and $TG_{L\ 2020}$, while there were many protein bands at the interface between the concentrated gel and the separated gel at the same time (Fig. 1E and F), indicating that the protein cross-linking took place. After incubation at 40 °C for 15 min, TG_{LD} converted most of the β-casein bands into cross-linked bands, whereas in the case of $TG_{L\ 2020}$, a clear β-casein band was still seen even after 30 min of reaction. Furthermore, the protein cross-linking efficiency of TG_{LD} was higher than that of TG_{L2020} at 50 °C. These results indicated that TG_{LD} had a high protein cross-linking efficiency compared with $TG_{L\ 2020}$. These were the main reasons that TG_{LD} had a higher catalytic efficiency and stability than those of $TG_{L\ 2020}$, indicating that TG_{LD} could be more widely used in food, textile, and pharmaceutical industries. However, the low yield of TG_{LD} in *S. mobaraensis* smLD limits its industrial application, and thus, further work is in need to enhance the production of TG_{LD}.

3.2. Increasing the expression level of tg_{LD} in S. mobaraensis smLD

The protein production can be increased by integrating multiple copy gene expression cassettes into the genome. As shown in Fig. 2, the initial activity of TG_{LD} in *S. mobaraensis* smLD was only 2.07 U/mL. Here, in order to increase the production of TG_{LD}, the plasmid pSET152 was used to integrate multiple copies of the tg_{LD} expression cassettes

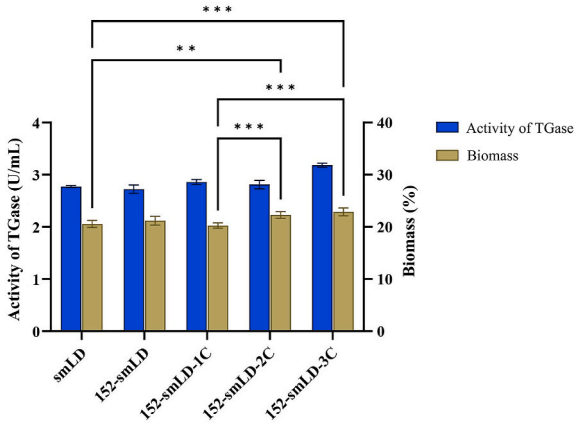

Fig. 2. Improving the expression level of tg_{LD} in *S. mobaraensis* smLD using multiple copies of tg_{LD} expression cassettes. smLD, *S. mobaraensis* smLD. 152-smLD, *S. mobaraensis* 152-smLD (The control). 152-smLD-1C, *S. mobaraensis* 152-smLD-1C. 152-smLD-2C, *S. mobaraensis* 152-smLD-2C. 152-smLD-3C, *S. mobaraensis* 152-smLD-3C.

(one, two, and three copies) into the gene site *attB* of the *S. mobaraensis* smLD genome to construct recombinant strains *S. mobaraensis* 152-smLD-1C, *S. mobaraensis* 152-smLD-2C, and *S. mobaraensis* 152-smLD-3C, respectively. The activity of TG_{LD} in *S. mobaraensis* 152-smLD-1C, *S. mobaraensis* 152-smLD-2C, and *S. mobaraensis* 152-smLD-3C reached 2.86, 2.81, and 3.18 U/mL, respectively. The expression level of TG_{LD} in *S. mobaraensis* smLD was enhanced by multiple copies of the tg_{LD} expression cassettes, and activity of TG_{LD} in *S. mobaraensis* 152-smLD-3C was 53.62% higher than that of the initial *S. mobaraensis* smLD. However, the activity of TG_{LD} in *S. mobaraensis* 152-smLD-3C was still not high for industrial production (Noda et al., 2012). Several *Streptomyces* spp. Have been used as the expression hosts for exogenous proteins, but the expression level was still low. The potential reasons might be homologous sources, heterologous hosts, and molecular tools (promoters/vectors/signal peptides) (Berini et al., 2020). In order to increase the industrial production of TG_{LD}, an ideal 'universal host' for TG heterologous expression was needed to construct by efficient

bioengineering strategies.

3.3. Deleting the gene tg_{L2020} from *S. mobaraensis* smL2020

The activity of TG_{L2020} in *S. mobaraensis* smL2020 reached 41.27 U/mL (Fig. 3A), the yield of extracellular TGase was 1.6 g/L, indicating that *S. mobaraensis* smL2020 might be a better expression and secretion system of TGase. In this study, *S. mobaraensis* smL2020 was used as a new expression host of TG_{LD} with perfected parameters (e.g., high catalytic efficiency, stability, and protein cross-linking efficiency). First, the plasmid pKC1132-*gfp-dTG* with a tg_{L2020} knockout cassette was constructed to delete the gene tg_{L2020} in *S. mobaraensis* smL 2020. Single and double crossovers were used to delete the gene tg_{L2020} in *S. mobaraensis* smL 2020. Positive double crossover colonies were characterized by determining fluorescence and apramycin resistance (Fig. 3B). Positive double crossover colonies were further verified by PCR (Fig. S3), and engineered *S. mobaraensis* smL2020ΔTG with tg_{L2020} deleted was obtained.

The TGase activity and cell growth of *S. mobaraensis* smL2020ΔTG were determined and compared. TGase activities of *S. mobaraensis* smL2020 were 19.83, 41.27, 40.72, and 37.23 U/mL at 24, 56, 60, and 64 h, respectively (Fig. 3C). However, no TGase activity of *S. mobaraensis* smL2020ΔTG was obtained at 24, 56, 60, and 64 h. Furthermore, no target bands of TGase were found for *S. mobaraensis* smL2020ΔTG by SDS-PAGE, which was consistent with the TGase activity (Fig. 3D). It was further verified that the gene tg_{L2020} in *S. mobaraensis* smL2020ΔTG had been deleted.

3.4. Enhancement of the heterologous expression of the gene tg_{LD} in *S. mobaraensis smL2020ΔTG*by optimizing signal peptides and promoters

The gene tg_{LD} from *S. mobaraensis* smLD with its natural signal peptide SP_{LD} was heterologously expressed in *S. mobaraensis* smL2020ΔTG, and *S. mobaraensis* smL2020ΔTG::P_{LD}-sp_{LD}-$protg_{LD}$-tg_{LD} was constructed. The activity of TGase in *S. mobaraensis* smL2020ΔTG::P_{LD}-sp_{LD}-$protg_{LD}$-tg_{LD} was 0.58 U/mL (Fig. 4), which was still low. The signal peptide, promoter, leader peptide, 5' untranslated region, and open reading frame are significant aspects of protein expression. It was found that expression levels of the papain inhibitor PI1 and subtilase-type protease inhibitor PI2 were higher than that of the zymogen pro-TG_{LD} and TG_{LD} in *S. mobaraensis* smLD (Fig. 4A). Here, in order to improve the production level of TG_{LD}, the signal peptide SP_{PI} of the papain inhibitor PI1 and the signal peptide SP_{SI} of the subtilase-type protease inhibitor PI2 were used to replace the signal peptide SP_{LD} of TG_{LD} in *S. mobaraensis* smL2020ΔTG::P_{LD}-sp_{LD}-$protg_{LD}$-tg_{LD}. Moreover, the signal peptide SP_{L2020} of TG_{L2020} was also used to replace the signal peptide SP_{LD} of TG_{LD} in *S. mobaraensis* smL2020ΔTG::P_{LD}-sp_{LD}-$protg_{LD}$-tg_{LD}. As shown in Fig. 4B, the activity of TG_{LD} in *S. mobaraensis* smL2020ΔTG::P_{LD}-sp_{L2020}-$protg_{LD}$-tg_{LD} reached 0.95 U/mL after incorporating the signal peptide SP_{L2020} of $TG_{L\ 2020}$, which was a 63.79% increase. However, the signal peptides SP_{PI} and SP_{SI} inhibited production of TG_{LD} in *S. mobaraensis* smL2020ΔTG. This indicated that signal peptide SP_{L2020} was important for enhancing the expression level of TG_{LD} in *S. mobaraensis* smL2020ΔTG.

Promoters are key factors affecting expression of recombinant proteins. There have been several strong promoters developed in

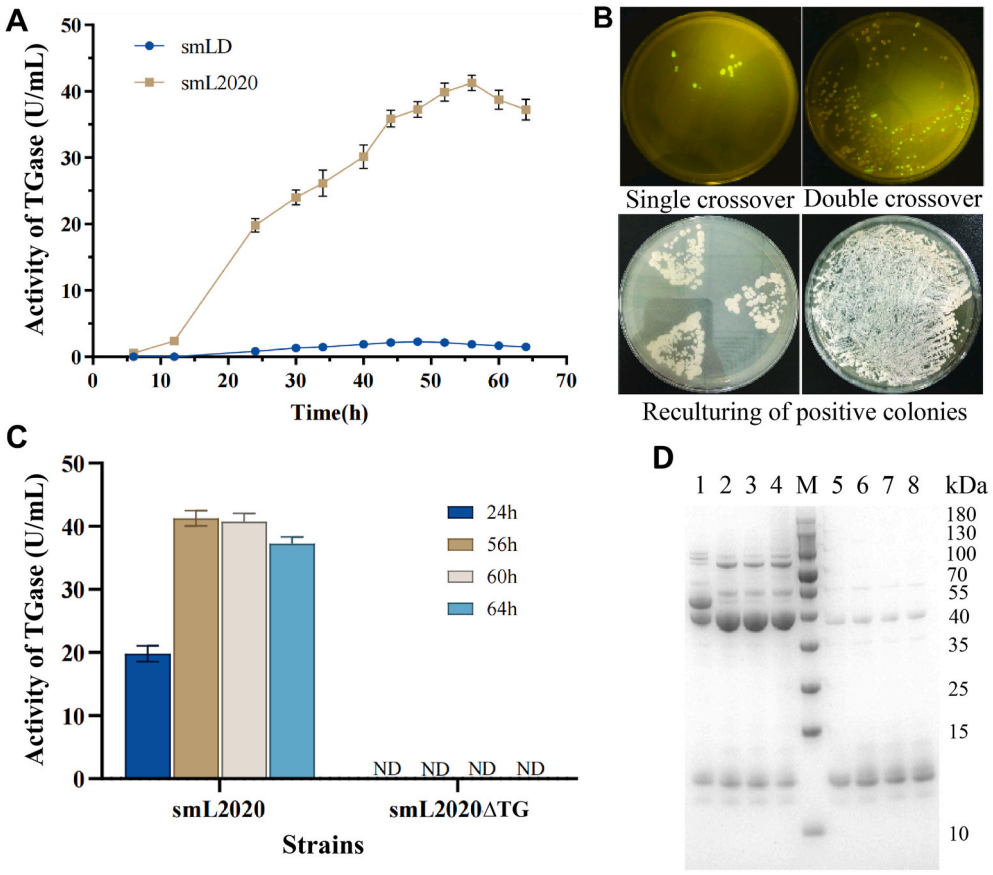

Fig. 3. Deleting the gene tg_{L2020} from *S. mobaraensis* smL 2020. A, Comparation of TGase activity between *S. mobaraensis* smLD and *S. mobaraensis* smL 2020. smLD, *S. mobaraensis* smLD. smL 2020, *S. mobaraensis* smL 2020. B, Comparation of single and double crossovers for efficiency of deleting gene tg_{L2020} in *S. mobaraensis* smL 2020. C, Verification of TGase production in *S. mobaraensis* smL2020ΔTG. smL 2020, *S. mobaraensis* smL 2020. smL2020ΔTG, *S. mobaraensis* smL2020ΔTG. D, SDS-PAGE of TGase production in *S. mobaraensis* smL2020ΔTG. M, Standard weight proteins (Marker). 1–4, *S. mobaraensis* smL 2020.1, 20 h. 2, 24 h. 3, 60 h. 4, 64 h. 5–8, *S. mobaraensis* smL2020ΔTG. 5, 20 h. 6, 24 h. 7, 60 h. 8, 64 h.

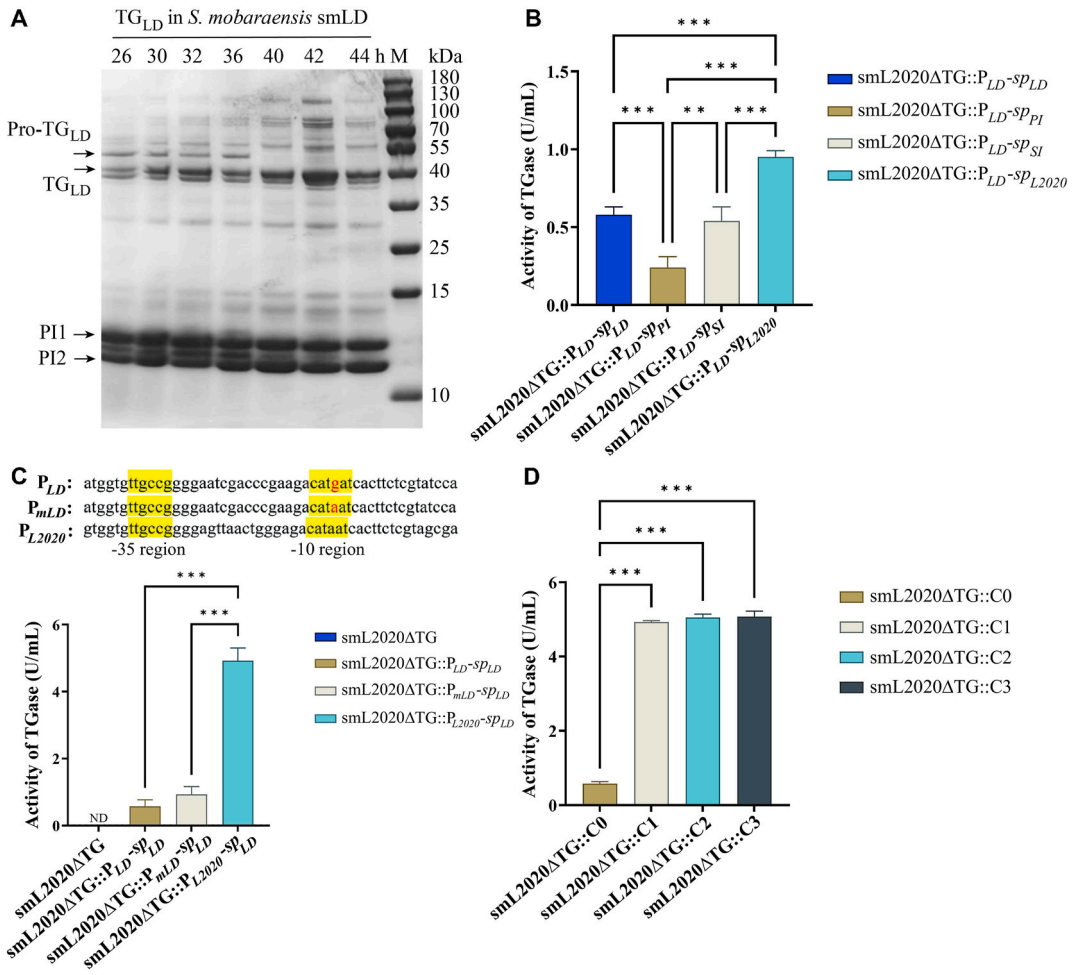

Fig. 4. Improving the heterologous expression level of tg_{LD} from *S. mobaraensis* smLD in *S. mobaraensis* smL2020ΔTG by optimizing signal peptides and promoter engineering. A, SDS-PAGE of TG_{LD} in *S. mobaraensis* smLD. M, Standard weight proteins (Marker). Pro-TG_{LD}, the zymogen Pro-TG_{LD}. PI1, the papain inhibitor PI1. PI2, the subtilase-type protease inhibitor PI2. B, Effect of different signal peptides on expression level of tg_{LD} in *S. mobaraensis* smL2020ΔTG. smL2020ΔTG::P_{LD}-sp_{LD}, *S. mobaraensis* smL2020ΔTG::P_{LD}-sp_{LD}-$protg_{LD}$-tg_{LD}. smL2020ΔTG::P_{LD}-sp_{PI}, *S. mobaraensis* smL2020ΔTG::P_{LD}-sp_{PI}-$protg_{LD}$-tg_{LD}. smL2020ΔTG::P_{LD}-sp_{SI}, *S. mobaraensis* smL2020ΔTG::P_{LD}-sp_{SI}-$protg_{LD}$-tg_{LD}. smL2020ΔTG::P_{LD}-sp_{L2020}, *S. mobaraensis* smL2020ΔTG::P_{LD}-sp_{L2020}-$protg_{LD}$-tg_{LD}. C, Effect of promoters P_{LD}, P_{mLD}, and P_{L2020} on expression level of tg_{LD} in *S. mobaraensis* smL2020ΔTG. smL2020ΔTG, *S. mobaraensis* smL2020ΔTG. smL2020ΔTG::P_{LD}-sp_{LD}, *S. mobaraensis* smL2020ΔTG::P_{LD}-sp_{LD}-$protg_{LD}$-tg_{LD}. smL2020ΔTG::P_{mLD}-sp_{LD}, *S. mobaraensis* smL2020ΔTG::P_{mLD}-sp_{LD}-$protg_{LD}$-tg_{LD}. smL2020ΔTG::P_{L2020}-sp_{LD}, *S. mobaraensis* smL2020ΔTG::P_{L2020}-sp_{LD}-$protg_{LD}$-tg_{LD}. D, Effect of different expression cassette on TG_{LD} activity in *S. mobaraensis* smL2020ΔTG. smL2020ΔTG::C0, *S. mobaraensis* smL2020ΔTG::P_{LD}-sp_{LD}-$protg_{LD}$-tg_{LD} (C0). smL2020ΔTG::C1, *S. mobaraensis* smL2020ΔTG::P_{L2020}-sp_{L}D-$protg_{LD}$-tg_{LD} (C1). smL2020ΔTG::C2, *S. mobaraensis* smL2020ΔTG::P_{L2020}-sp_{L2020}-$protg_{LD}$-tg_{LD} (C2). smL2020ΔTG::C3, *S. mobaraensis* smL2020ΔTG::P_{L2020}-sp_{L2020}-$protg_{L}$2020-tg_{LD} (C3). **, p value < 0.01. ***, p value < 0.001.

Streptomyces, including P_{kasOp*}, P_{21}, and P_{ermE*} (Doumith et al., 2000; Siegl et al., 2013; Wang et al., 2013). Mutations in the −10 region of promoters can induce significant changes in the expression level of recombinant proteins. In order to study and identify the main reason that the expression level of tg_{L2020} was higher than that of tg_{LD}, the −10 regions of promoters P_{LD} and P_{L2020} were blasted and analyzed. It was found that one base in the −10 region of the promoters P_{LD} and P_{L2020} were different (Fig. 4C). In this study, a G base in the −10 region of TG_{LD} promoter P_{LD} was replaced by an A base, named P_{mLD}. Promoter P_{LD} in *S. mobaraensis* smL2020ΔTG::P_{LD}-sp_{LD}-$protg_{LD}$-tg_{LD} was replaced by P_{mLD} to construct *S. mobaraensis* smL2020ΔTG::P_{mLD}-sp_{LD}-$protg_{LD}$-tg_{LD}. The activity of TG_{LD} in *S. mobaraensis* smL2020ΔTG::P_{mLD}-sp_{LD}-$protg_{LD}$-tg_{LD} reached 0.93 U/mL, indicating a 1.6-fold increase over that of *S. mobaraensis* smL2020ΔTG::P_{LD}-sp_{LD}-$protg_{LD}$-tg_{LD} (Fig. 4C). This indicated that the A base in the −10 region of the TG_{LD} promoter P_{LD} was important for enhancing the expression level of TG_{LD} in *S. mobaraensis* smL2020ΔTG, which was in accordance with previous reports (Phan et al., 2012; Zhou et al., 2019). It was also found that the expression level of proteins was significantly affected by mutating several bases in the −10 region of the promoters. Additionally, the promoter P_{LD} of *S. mobaraensis* smL2020ΔTG::P_{LD}-sp_{LD}-$protg_{LD}$-tg_{LD} was replaced by the promoter P_{L2020} to construct *S. mobaraensis* smL2020ΔTG::P_{L2020}-sp_{LD}-$protg_{LD}$-tg_{LD}. Promoter P_{L2020} significantly enhanced production of TG_{LD} in *S. mobaraensis* smL2020ΔTG. Activity of TG_{LD} in *S. mobaraensis* smL2020ΔTG::P_{L2020}-sp_{LD}-$protg_{LD}$-tg_{LD} reached 4.92 U/mL, indicating a 4.29-fold increase over that of *S. mobaraensis* smL2020ΔTG::P_{mLD}-sp_{LD}-$protg_{LD}$-tg_{LD}. This verified that promoter P_{L2020} was preferred to promoters P_{LD} and P_{mLD} for expression of TG_{LD} in *S. mobaraensis* smL2020ΔTG.

Based on the above optimal elements (promoter and signal peptide), *S. mobaraensis* smL2020ΔTG::P_{L2020}-sp_{L2020}-$protg_{LD}$-tg_{LD} was constructed (Fig. 4D). The activity of TG_{LD} in *S. mobaraensis* smL2020ΔTG::P_{L2020}-sp_{L2020}-$protg_{LD}$-tg_{LD} (C2) reached 5.05 U/mL, suggesting an 8.71-fold increase over that of *S. mobaraensis* smL2020ΔTG::P_{LD}-sp_{LD}-$protg_{LD}$-tg_{LD} (C0). This indicated that the promoter P_{L2020} and signal peptide SP_{L2020} were significant for production of TG_{LD} in *S. mobaraensis* smL2020ΔTG. In order to further improve the production level of TG_{LD}, the natural propeptide gene $protg_{LD}$ of TG_{LD} in *S. mobaraensis* smL2020ΔTG::P_{L2020}-sp_{LD}-$protg_{LD}$-tg_{LD} was replaced by the propeptide gene $protg_{L2020}$ of TG_{L2020}, and *S. mobaraensis* smL2020ΔTG::P_{L2020}-sp_{L2020}-$protg_{L2020}$-tg_{LD} was

constructed. The activity of TG_{LD} in *S. mobaraensis* smL2020ΔTG::P_{L2020}-sp_{L2020}-$protg_{L2020}$-tg_{LD} (C3) reached 5.07 U/mL, indicating an 8.74-fold increase over that of *S. mobaraensis* smL2020ΔTG::P_{LD}-sp_{LD}-$protg_{LD}$-tg_{LD} (C0). These results showed that the promoter P_{L2020} was more important for production of TG_{LD} in *S. mobaraensis* smL2020ΔTG than the signal peptides.

3.5. Enhancement of the heterologous expression of the gene tg_{LD} in *S. mobaraensis* smL2020ΔTG by increasing copies of the expression cassettes of tg_{LD}

It has been verified that integration of multiple genes into the genome increased protein production level (He et al., 2016). The effect of multiple copies of the expression cassettes on the expression level of tg_{LD} in *S. mobaraensis* smL2020ΔTG was studied (Fig. 5). First, two and three copies of the tg_{LD} expression cassette P_{LD}-sp_{LD}-$protg_{LD}$-tg_{LD} from *S. mobaraensis* smLD were transformed into *S. mobaraensis* smL2020ΔTG to construct *S. mobaraensis* smL2020ΔTG: $(P_{LD}$-sp_{LD}-$protg_{LD}$-$tg_{LD})_2$ and *S. mobaraensis* smL2020ΔTG: $(P_{LD}$-sp_{LD}-$protg_{LD}$-$tg_{LD})_3$, respectively. The activities of TG_{LD} in *S. mobaraensis* smL2020ΔTG: $(P_{LD}$-sp_{LD}-$protg_{LD}$-$tg_{LD})_2$ and *S. mobaraensis* smL2020ΔTG: $(P_{LD}$-sp_{LD}-$protg_{LD}$-$tg_{LD})_3$ reached 1.52 and 2.49 U/mL, indicating increases of 2.62- and 4.29-fold over that of *S. mobaraensis* smL2020ΔTG::P_{LD}-sp_{LD}-$protg_{LD}$-tg_{LD}, respectively. This suggested that production of TG_{LD} in *S. mobaraensis* smL2020ΔTG was strongly enhanced by multiple copies of the expression cassette. Additionally, two and three copies of the tg_{LD} expression cassette P_{mLD}-sp_{LD}-$protg_{LD}$-tg_{LD} were transformed into *S. mobaraensis* smL2020ΔTG to construct *S. mobaraensis* smL2020ΔTG: $(P_{mLD}$-sp_{LD}-$protg_{LD}$-$tg_{LD})_2$ and *S. mobaraensis* smL2020ΔTG: $(P_{mLD}$-sp_{LD}-$protg_{LD}$-$tg_{LD})_3$, respectively. The activities of TG_{LD} in *S.*

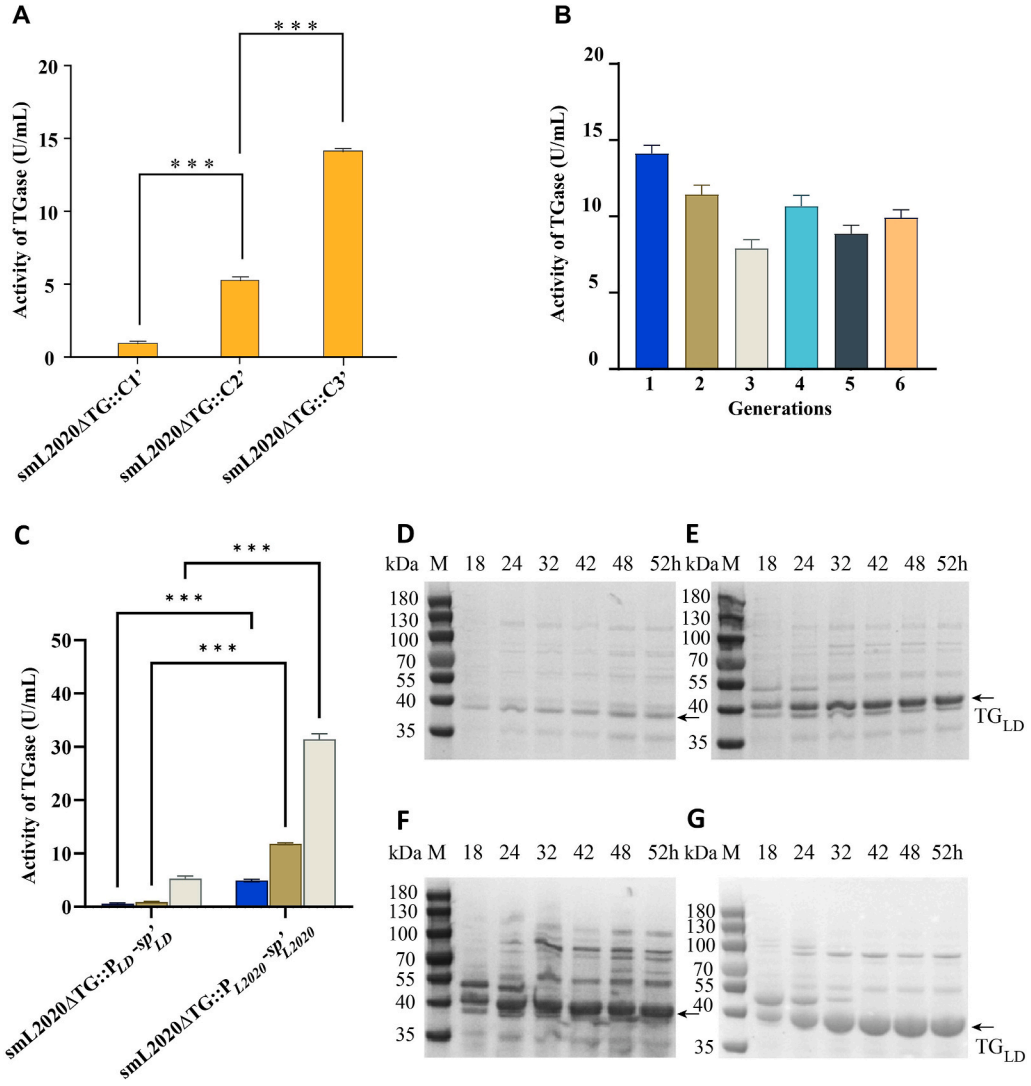

Fig. 5. Improving the heterologous expression level of tg_{LD} from *S. mobaraensis* smLD in *S. mobaraensis* smL2020ΔTG by increasing copies of the expression cassettes of tg_{LD} and effects of different recombination sites on the production level of tg_{LD} from *S. mobaraensis* smLD in *S. mobaraensis* smL2020ΔTG. A, Effect of different copies of the expression cassettes of tg_{LD} on TG_{LD} activity in *S. mobaraensis* smL2020ΔTG. smL2020ΔTG::C1′, *S. mobaraensis* smL2020ΔTG::P_{mLD}-sp_{LD}-$protg_{LD}$-tg_{LD}. smL2020ΔTG::C2′, *S. mobaraensis* smL2020ΔTG: $(P_{mLD}$-sp_{LD}-$protg_{LD}$-$tg_{LD})_2$. smL2020ΔTG::C3′, *S. mobaraensis* smL2020ΔTG: $(P_{mLD}$-sp_{LD}-$protg_{LD}$-$tg_{LD})_3$. B, The genetic stability of *S. mobaraensis* smL2020ΔTG: $(P_{mLD}$-sp_{LD}-$protg_{LD}$-$tg_{LD})_3$. C, Effects of different recombination sites on the production level of tg_{LD} from *S. mobaraensis* smLD in *S. mobaraensis* smL2020ΔTG. smL2020ΔTG::P_{LD}-sp'_{LD}, *S. mobaraensis* smL2020ΔTG::P_{LD}-sp_{LD}-$protg_{LD}$-tg_{LD} (blue column), *S. mobaraensis* smL2020ΔTG::P_{LD}-sp_{LD}-$protg_{LD}$-tg_{LD} (BT1) (dark yellow column), and *S. mobaraensis* smL2020ΔTG::P_{LD}-sp_{LD}-$protg_{LD}$-tg_{LD} ($tg_{L\ 2020}$) (light gray column). smL2020ΔTG::P_{L2020}-sp'_{L2020}, *S. mobaraensis* smL2020ΔTG::P_{L2020}-sp_{L2020}-$protg_{LD}$-tg_{LD} (blue column), *S. mobaraensis* smL2020ΔTG::P_{L2020}-sp_{L2020}-$protg_{LD}$-tg_{LD} (BT1) (dark yellow column), and *S. mobaraensis* smL2020ΔTG::P_{L2020}-sp_{L2020}-$protg_{LD}$-tg_{LD} ($tg_{L\ 2020}$) (light gray column). D, SDS-PAGE of TG_{LD} in *S. mobaraensis* smL2020ΔTG::P_{LD}-sp_{LD}-$protg_{LD}$-tg_{LD}. E, SDS-PAGE of TG_{LD} in *S. mobaraensis* smL2020ΔTG::P_{L2020}-sp_{L2020}-$protg_{LD}$-tg_{LD}. F, SDS-PAGE of TG_{LD} in *S. mobaraensis* smL2020ΔTG::P_{L2020}-sp_{L2020}-$protg_{LD}$-tg_{LD} (BT1). G, SDS-PAGE of TG_{LD} in *S. mobaraensis* smL2020ΔTG::P_{L2020}-sp_{L2020}-$protg_{LD}$-tg_{LD} ($tg_{L\ 2020}$). M, Standard weight proteins (Marker). ***, p value < 0.001.

mobaraensis smL2020ΔTG: (P_{mLD}-sp_{LD}-$protg_{LD}$-tg_{LD})$_2$ and *S. mobaraensis* smL2020ΔTG: (P_{mLD}-sp_{LD}-$protg_{LD}$-tg_{LD})$_3$ reached 5.26 and 14.13 U/mL, indicating 5.66- and 15.19-fold increases over that of *S. mobaraensis* smL2020ΔTG::P_{mLD}-sp_{LD}-$protg_{LD}$-tg_{LD}, respectively. The activity of TG_{LD} in *S. mobaraensis* smL2020ΔTG: (P_{mLD}-sp_{LD}-$protg_{LD}$-tg_{LD})$_3$ was 24.36-fold that of *S. mobaraensis* smL2020ΔTG::P_{LD}-sp_{LD}-$protg_{LD}$-tg_{LD}. It was further verified that multiple copies of the expression cassette were significant for efficient production of TG_{LD} in *S. mobaraensis* smL2020ΔTG, and that for the efficient production of TG_{LD} in *S. mobaraensis* smL2020ΔTG, promoter P_{mLD} was preferred to promoter P_{LD}. Yin et al. (2021) also found that TGase activity of smY 2019-3C with three copies of the TGase expression cassette was 103% higher than that of the control (smY 2019). The genetic stability of microorganism strains is important for their industrial application, and it reflects any potential mutations at the gene level (Ma et al., 2015).

However, activity of TG_{LD} in *S. mobaraensis* smL2020ΔTG: (P_{mLD}-sp_{LD}-$protg_{LD}$-tg_{LD})$_3$ decreased during a six-generation culture (Fig. 5B). This indicated that the genetic stability of *S. mobaraensis* smL2020ΔTG: (P_{mLD}-sp_{LD}-$protg_{LD}$-tg_{LD})$_3$ was not high. The main reason might be that the concatenated expression cassettes of TG_{LD} were partially lost during culture.

3.6. Effects of different recombination sites on the activity of TG_{LD}

Site-specific recombination was used to exchange two DNA molecules at predefined sites through integration, deletion, and reversal (Grindley et al., 2006). Bacteriophage-encoded serine recombinases have great potential for genetic engineering of *S. mobaraensis*. For site-specific recombination, several significant serine recombinases have an unusually large C-terminal DNA binding and recognition domain (Zhang et al., 2010). The most-studied large serine recombinases include integrases from *Streptomyces* phages BT1 and ΦC31, and from mycobacteriophages Bxb1 and ΦRv1 (Nkrumah et al., 2006; Zhang et al., 2008, 2010). It was found that BT1 and ΦC31 integrases cleaved single-substrate *att* sites (Zhang et al., 2010). In this study, two site-specific recombination systems (BT1 and ΦC31) that had different recombination sites were used for site-specific recombination. Plasmid pSET156 included the site-specific recombination system BT1, and plasmid pSET152 included the site-specific recombination system ΦC31. The expression cassette P_{LD}-sp_{LD}-$protg_{LD}$-tg_{LD} was integrated into the genome of *S. mobaraensis* smL2020ΔTG using plasmids pSET156 and pSET152 to construct the engineered strains *S. mobaraensis* smL2020ΔTG::P_{LD}-sp_{LD}-$protg_{LD}$-tg_{LD} (BT1) and *S. mobaraensis* smL2020ΔTG::P_{LD}-sp_{LD}-$protg_{LD}$-tg_{LD}, respectively. The activity of TG_{LD} in *S. mobaraensis* smL2020ΔTG::P_{LD}-sp_{LD}-$protg_{LD}$-tg_{LD} (BT1) increased 1.79-fold compared to that in *S. mobaraensis* smL2020ΔTG::P_{LD}-sp_{LD}-$protg_{LD}$-tg_{LD} (Fig. 5C). The expression cassette P_{L2020}-sp_{L2020}-$protg_{LD}$-tg_{LD} was integrated into the genome of *S. mobaraensis* smL2020ΔTG using plasmids pSET156 and pSET152 to construct the engineered strains *S. mobaraensis* smL2020ΔTG::P_{L2020}-sp_{L2020}-$protg_{LD}$-tg_{LD} (BT1) and *S. mobaraensis* smL2020ΔTG::P_{L2020}-sp_{L2020}-$protg_{LD}$-tg_{LD}, respectively. The activity of TG_{LD} in *S. mobaraensis* smL2020ΔTG::P_{L2020}-sp_{L2020}-$protg_{LD}$-tg_{LD} (BT1) reached 11.68 U/mL, which marked a 2.31-fold increase over that in *S. mobaraensis* smL2020ΔTG::P_{L2020}-sp_{L2020}-$protg_{LD}$-tg_{LD} (Fig. 5C). This verified that for TG_{LD} production in *S. mobaraensis* smL2020ΔTG, the recombination site of the site-specific recombination system BT1 was preferred to the recombination site of the site-specific recombination system ΦC31. The main reason might be that the recombination site of the site-specific recombination system ΦC31 was located in the gene of the redox-sensitive bicupin YhaK, and insertion of the expression cassettes destroyed this gene expression to change the metabolism of the strains (Gurmu et al., 2009).

Additionally, homologous recombination technology was used to insert expression cassettes P_{LD}-sp_{LD}-$protg_{LD}$-tg_{LD} and P_{L2020}-sp_{L2020}-$protg_{LD}$-tg_{LD} into the tg_{L2020} gene site of *S. mobaraensis* smL2020 to construct the engineered strains *S. mobaraensis* smL2020ΔTG::P_{LD}-sp_{LD}-$protg_{LD}$-tg_{LD} ($tg_{L\ 2020}$) and *S. mobaraensis* smL2020ΔTG::P_{L2020}-sp_{L2020}-$protg_{LD}$-tg_{LD} ($tg_{L\ 2020}$), respectively. The activity of TG_{LD} in *S. mobaraensis* smL2020ΔTG::P_{LD}-sp_{LD}-$protg_{LD}$-tg_{LD} ($tg_{L\ 2020}$) was 5.27 U/mL, signifying a 2.54-fold increase over that of the initial *S. mobaraensis* smLD (Fig. 5C). Therefore, *S. mobaraensis* smL2020 was preferred to *S. mobaraensis* smLD for the production of TGases. The activity of TG_{LD} in *S. mobaraensis* smL2020ΔTG::P_{LD}-sp_{LD}-$protg_{LD}$-tg_{LD} ($tg_{L\ 2020}$) increased 5.07- and 9.09-fold over that of *S. mobaraensis* smL2020ΔTG::P_{LD}-sp_{LD}-$protg_{LD}$-tg_{LD} (BT1) and *S. mobaraensis* smL2020ΔTG::P_{LD}-sp_{LD}-$protg_{LD}$-tg_{LD}, respectively. Therefore, for TG_{LD} production, the homologous recombination of the expression cassettes in the tg_{L2020} gene site was preferred to the recombination sites of site-specific recombination systems (BT1 and ΦC31).

Moreover, the activity of TG_{LD} in *S. mobaraensis* smL2020ΔTG::P_{L2020}-sp_{L2020}-$protg_{LD}$-tg_{LD} ($tg_{L\ 2020}$) was significantly enhanced compared with that of *S. mobaraensis* smL2020ΔTG::P_{L2020}-sp_{L2020}-$protg_{LD}$-tg_{LD} (BT1) and *S. mobaraensis* smL2020ΔTG::P_{L2020}-sp_{L2020}-$protg_{LD}$-tg_{LD}. The activity of TG_{LD} in *S. mobaraensis* smL2020ΔTG::P_{L2020}-sp_{L2020}-$protg_{LD}$-tg_{LD} ($tg_{L\ 2020}$) reached 31.18 U/mL, which indicated a 53.75-fold increase over that of *S. mobaraensis* smL2020ΔTG::P_{LD}-sp_{LD}-$protg_{LD}$-tg_{LD}. This was also verified by SDS-PAGE (Fig. 5D/E/F/G). It was further verified that the homologous recombination of the expression cassettes at the tg_{L2020} gene site was preferred to the recombination sites of the site-specific recombination systems (BT1 and ΦC31).

3.7. Enhancement of the tg_{LD} expression by increasing the copy number of the expression cassette P_{L2020}-sp_{L2020}-$protg_{LD}$-tg_{LD}

To further improve the expression level of the gene tg_{LD}, a site-specific recombination system (BT1) was used to integrate a second expression cassette P_{L2020}-sp_{L2020}-$protg_{LD}$-tg_{LD} into the genome of *S. mobaraensis* smL2020ΔTG::P_{L2020}-sp_{L2020}-$protg_{LD}$-tg_{LD} ($tg_{L\ 2020}$) to construct the engineered strain *S. mobaraensis* smL2020ΔTG: (P_{L2020}-sp_{L2020}-$protg_{LD}$-tg_{LD})$_2$ (tg_{L2020} and BT1). The activity of TG_{LD} in *S. mobaraensis* smL2020ΔTG: (P_{L2020}-sp_{L2020}-$protg_{LD}$-tg_{LD})$_2$ (tg_{L2020} and BT1) reached 56.43 U/mL in a 250-mL flask, indicating a 97.3-fold increase over that of *S. mobaraensis* smL2020ΔTG::P_{LD}-sp_{LD}-$protg_{LD}$-tg_{LD} (Fig. 6A).

Moreover, activity of TG_{LD} in *S. mobaraensis* smL2020ΔTG: (P_{L2020}-sp_{L2020}-$protg_{LD}$-tg_{LD})$_2$ (tg_{L2020} and BT1) did not decrease during 20 generations of culture (Fig. 6B). This indicated that the genetic stability of *S. mobaraensis* smL2020ΔTG: (P_{L2020}-sp_{L2020}-$protg_{LD}$-tg_{LD})$_2$ (tg_{L2020} and BT1) was high. It was concluded that *S. mobaraensis* smL2020ΔTG: (P_{L2020}-sp_{L2020}-$protg_{LD}$-tg_{LD})$_2$ (tg_{L2020} and BT1) has great potential for the industrial production of TG_{LD}.

3.8. Biosynthesis of TG_{LD} in *S. mobaraensis sml2020ΔTG*: (P_{L2020}-sp_{l2020}-$protg_{LD}$-tg_{LD})$_2$ (tg_{L2020} and BT1) in a 1000-L fermentor

In order to verify the potential for industrial production, TG_{LD} in *S. mobaraensis* smL2020ΔTG: (P_{L2020}-sp_{L2020}-$protg_{LD}$-tg_{LD})$_2$ (tg_{L2020} and BT1) was synthesized in a 1000-L fermentor (Fig. 6C). The activity of TG_{LD} in *S. mobaraensis* smL2020ΔTG: (P_{L2020}-sp_{L2020}-$protg_{LD}$-tg_{LD})$_2$ (tg_{L2020} and BT1) slowly increased before 20 h, and then quickly increased between 24 and 30 h. The activity of TG_{LD} in *S. mobaraensis* smL2020ΔTG: (P_{L2020}-sp_{L2020}-$protg_{LD}$-tg_{LD})$_2$ (tg_{L2020} and BT1) reached a maximum (63.18 U/mL) at 42 h in the 1000-L fermentor, which was the highest activity reported to date. In a previous study, random mutagenesis and site-directed genetic modifications were used to improve the production of TGase in *S. mobaraensis*, the activity of which reached 40 U/mL in a flask (Yin et al., 2021). The protein concentration of TG_{LD} produced in *S. mobaraensis* smL2020ΔTG: (P_{L2020}-sp_{L2020}-$protg_{LD}$-tg_{LD})$_2$ (tg_{L2020} and BT1) reached approximately 1.7 g/L. This was also verified by SDS-PAGE (Fig. 6D). A large amount of the zymogen pro-TG_{LD} accumulated during 0–24 h, most of which was transformed to mature

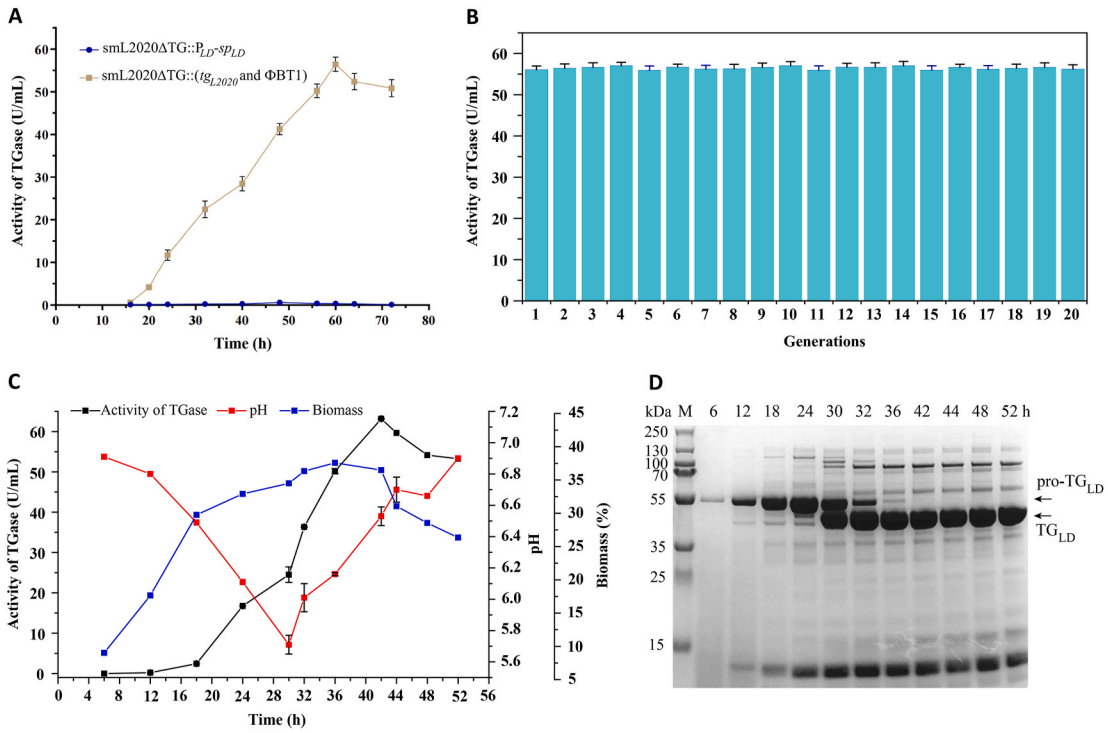

Fig. 6. Effect of increasing the copy number of the expression cassette P_{L2020}-sp_{L2020}-$protg_{LD}$-tg_{LD} on improving heterologous expression levels of tg_{LD} in *S. mobaraensis* smL2020ΔTG::P_{L2020}-sp_{L2020}-$protg_{LD}$-tg_{LD} ($tg_{L\ 2020}$) and production of TG_{LD} in *S. mobaraensis* smL2020ΔTG: (P_{L2020}-sp_{L2020}-$protg_{LD}$-tg_{LD})$_2$ (tg_{L2020} and BT1) in a 1000-L fermentor. A, Effect of increasing the copy number of the expression cassette P_{L2020}-sp_{L2020}-$protg_{LD}$-tg_{LD} on improving heterologous expression levels of tg_{LD} in *S. mobaraensis* smL2020ΔTG::P_{L2020}-sp_{L2020}-$protg_{LD}$-tg_{LD} ($tg_{L\ 2020}$). B, The genetic stability of *S. mobaraensis* smL2020ΔTG: (P_{L2020}-sp_{L2020}-$protg_{LD}$-tg_{LD})$_2$ (tg_{L2020} and BT1). C, Production of TG_{LD} in *S. mobaraensis* smL2020ΔTG: (P_{L2020}-sp_{L2020}-$protg_{LD}$-tg_{LD})$_2$ (tg_{L2020} and BT1) in a 1000-L fermentor. D, SDS-PAGE of TG_{LD} in *S. mobaraensis* smL2020ΔTG: (P_{L2020}-sp_{L2020}-$protg_{LD}$-tg_{LD})$_2$ (tg_{L2020} and BT1) in a 1000-L fermentor. M, Standard weight proteins (Marker).

TG_{LD} at 30 h. All of the zymogen proTGase was transformed to mature TG_{LD} by 42 h, which was consistent with the change in TG_{LD} activity. The cell density of *S. mobaraensis* smL2020ΔTG: (P_{L2020}-sp_{L2020}-$protg_{LD}$-tg_{LD})$_2$ (tg_{L2020} and BT1) progressively increased from 0 to 24 h, and reached a maximum at 36 h. This further verified that *S. mobaraensis* smL2020ΔTG: (P_{L2020}-sp_{L2020}-$protg_{LD}$-tg_{LD})$_2$ (tg_{L2020} and BT1) has great potential for industrial production of TG_{LD}.

4. Conclusions

In summary, systematic engineering strategies were used to construct a recombinant *S. mobaraensis* strain with high industrial productivity of TGase and perfected characteristics in a 1000-L fermentor. Compared with TG_{L2020} from *S. mobaraensis* sm 2020, TG_{LD} from *S. mobaraensis* smLD had better parameters (e.g., high catalytic efficiency, stability, and protein cross-linking efficiency), which indicated that TG_{LD} had wider applications in food industry, especially in the case of low-quality raw materials (e.g. PSE meat or mechanically recovered meat). In this study, multiple copies of the tg_{LD} expression cassette and optimization of promoter and signal were used to increase the expression levels of TG_{LD}, but its activity was still not sufficiently high for industrial production. Finally, using the tg_{L2020} gene site and recombination sites of the site-specific recombination system BT1 to express two copies of the expression cassettes P_{L2020}-sp_{L2020}-$protg_{LD}$-tg_{LD}, the final TG_{LD} activity in the recombinant *S. mobaraensis* smL2020ΔTG: (P_{L2020}-sp_{L2020}-$protg_{LD}$-tg_{LD})$_2$ (tg_{L2020} *and* BT1) reached 56.43 U/mL and 63.18 U/mL in shake flask and 1000-L fermentor, respectively, and the genetic stability of this strain was high. The expression of TG_{LD} on the *Streptomyces* genome was affected by potential positional effects, suggesting that looking for better gene locations on the genome to integrate the TGase gene will further increase its yield and potential for industrialization.

CRediT authorship contribution statement

Fang Yuan: wrote the manuscript, performed research, drew figures. **Guoying Li:** wrote the manuscript, performed research, drew figures. **Zilong Li:** designed the manuscript, Writing – review & editing. **Mingming Li:** designed the manuscript, performed research. **Xiaobo Liu:** designed the manuscript, Writing – review & editing. **Haiquan Yang:** designed, Writing – review & editing, drew figures, All authors read and approved the manuscript. **Xiaobin Yu:** designed the manuscript, Writing – review & editing.

Declaration of competing interest

The authors declare that they have no known competing financial interests or personal relationships that could have appeared to influence the work reported in this paper.

Data availability

Data will be made available on request.

Acknowledgements

This work was funded by the Jiangsu Province 111 Project (Grant no.: 111-2-06).

Appendix A. Supplementary data

Supplementary data to this article can be found online at https://doi.org/10.1016/j.crfs.2024.100756.

References

Ando, H., Adachi, M., Umeda, K., Matsuura, A., Nonaka, M., Uchio, R., Tanaka, H., Motoki, M., 1989. Purification and characteristics of a novel transglutaminase derived from microorganisms. Agric. Biol. Chem. 53 (10), 2613–2617. https://doi.org/10.1080/00021369.1989.10869735.

Bagagli, M.P., Sato, H.H., 2013. Two-staged temperature and agitation strategy for the production of transglutaminase from a *Streptomyces sp*. isolated from Brazilian soils. Appl. Biochem. Biotechnol. 170 (5), 1057–1065. https://doi.org/10.1007/s12010-013-0251-x.

Bauer, C., Osman, A.M., Cercignani, G., Gialluca, N., Paolini, M., 2001. A unified theory of enzyme kinetics based upon the systematic analysis of the variations of k_{cat}, K_M, and k_{cat}/K_M and the relevant $\Delta G0\neq$ values—possible implications in chemotherapy and biotechnology. Biochem. Pharmacol. 61 (9), 1049–1055. https://doi.org/10.1016/s0006-2952(01)00579-2.

Berini, F., Marinelli, F., Binda, E., 2020. *Streptomycetes*: attractive hosts for recombinant protein production. Front. Microbiol. 11 https://doi.org/10.3389/fmicb.2020.01958.

Bierman, M., Logan, R., O'Brien, K., Seno, E.T., Rao, R.N., Schoner, B.E., 1992. Plasmid cloning vectors for the conjugal transfer of DNA from *Escherichia coli* to *Streptomyces* spp. Gene116(1) 43–49. https://doi.org/10.1016/0378-1119(92)90627-2.

Cui, L., Du, G., Zhang, D., Chen, J., 2008. Thermal stability and conformational changes of transglutaminase from a newly isolated *Streptomyces hygroscopicus*. Bioresour. Technol. 99 (9), 3794–3800. https://doi.org/10.1016/j.biortech.2007.07.017.

Doumith, M., Weingarten, P., Wehmeier, U.F., Salah-Bey, K., Benhamou, B., Capdevila, C., Michel, J.M., Piepersberg, W., Raynal, M.C., 2000. Analysis of genes involved in 6-deoxyhexose biosynthesis and transfer in Saccharopolyspora erythraea. Mol. Genet. Genom. 264 (4), 477–485. https://doi.org/10.1007/s004380000329.

Duarte, L.S., Matte, C.R., Bizarro, C.V., Ayub, M.A.Z., 2020. Review transglutaminases: part II—industrial applications in food, biotechnology, textiles and leather products. Biotechnol. Bioproc. Biocatal. 36 (1), 1–20. https://doi.org/10.1007/s11274-019-2792-9.

Esmaeilnejad-Ahranjani, P., Hajimoradi, M., 2022. Optimization of industrial-scale centrifugal separation of biological products: comparing the performance of tubular and disc stack centrifuges. Biochem. Eng. J. 178, 108281 https://doi.org/10.1016/j.bej.2021.108281.

Evanthia Monogioudi, N.C., Kruus, Kristiina, Gruppen, Harry, Buchert, Johanna, Mattinen, Maija-Liisa, 2009. Cross-linking of β-casein by *Trichoderma reesei* tyrosinase and *Streptoverticillium mobaraense* transglutaminase followed by SEC–MALLS. Food Hydrocolloids 23 (7), 2008–2015. https://doi.org/10.1016/j.foodhyd.2009.03.011.

Fernandes, C.G., Martins, D., Hernandez, G., Sousa, A.L., Freitas, C., Tranfield, E.M., Cordeiro, T.N., Serrano, M., Moran, C.P., Henriques, A.O., 2019. Temporal and spatial regulation of protein cross-linking by the pre-assembled substrates of a *Bacillus subtilis* spore coat transglutaminase. PLoS Genet. 15 (4), e1007912 https://doi.org/10.1371/journal.pgen.1007912.

Folk, J.E., Cole, P.W., 1966. Transglutaminase: Mechanistic features of the active site as determined by kinetic and inhibitor studies. Publ. Health Serv. 122 (2), 244–264. https://doi.org/10.1016/0926-6593(66)90066-x.

Gil, J.A., Kieser, H.M., Hopwood, D.A., 1985. Cloning of a chloramphenicol acetyltransferase gene of *Streptomyces acrimycini* and its expression in *Streptomyces* and *Escherichia coli*. Gene. 38 (1–3), 1–8. https://doi.org/10.1016/0378-1119(85)90197-0.

Grindley, N.D.F., Whiteson, K.L., Rice, P.A., 2006. Mechanisms of site-specific recombination. Annu. Rev. Biochem. 75 (1), 567–605.. https://doi.org/10.1146/annurev.biochem.73.011303.073908.

Gurmu, D., Lu, J., Johnson, K.A., Nordlund, P., Holmgren, A., Erlandsen, H., 2009. The crystal structure of the protein YhaK from *Escherichia coli* reveals a new subclass of redox sensitive enterobacterial bicupins. Proteins: Struct., Funct., Genet. 74 (1), 18–31. https://doi.org/10.1002/prot.22128.

He, W., Mu, W., Jiang, B., Yan, X., Zhang, T., 2016. Food-grade expression of D-Psicose 3-epimerase with tandem repeat genes in *Bacillus subtilis*. J. Agric. Food Chem. 64 (28), 5701–5707. https://doi.org/10.1021/acs.jafc.6b02209.

Jiang, Y., Shang, Y., Li, H., Zhang, C., Pan, J., Bai, Y., Li, C., Xu, J., 2017. Enhancing transglutaminase production of *Streptomyces mobaraensis* by iterative mutagenesis breeding with atmospheric and room-temperature plasma (ARTP). Bioresour. Bioprocess. 4 (1), 37. https://doi.org/10.1186/s40643-017-0168-2.

Kashiwagi, T., Yokoyama, K.-I., Ishikawa, K., Ono, K., Ejima, D., Matsui, H., Suzuki, E.-i., 2002. Crystal structure of microbial transglutaminase from *Streptoverticillium mobaraense*. J. Biol. Chem. 277 (46), 44252–44260. https://doi.org/10.1074/jbc.M203933200.

Kobayashi, K., Hashiguchi, K.-I., Yokozeki, K., Yamanaka, S., 1998. Molecular cloning of the transglutaminase gene from *Bacillus Subtilis* and its expression in *Escherichia coli*. Biosci. Biotechnol. 62 (6), 1109–1114. https://doi.org/10.1271/bbb.62.1109.

Lorenzen, P.C., 2008. Effects of varying time/temperature-conditions of pre-heating and enzymatic cross-linking on techno-functional properties of reconstituted dairy ingredients. Food Res. Int. 40 (6), 700–708. https://doi.org/10.1016/j.foodres.2006.12.001.

Lu, S., Zhou, N., Tian, Y., Li, H., Chen, J., 2003. Purification and properties of transglutaminase from *Streptoverticillium mobaraense*. J. Food Biochem. 27 (2), 109–125. https://doi.org/10.1111/j.1745-4514.2003.tb00270.x.

Luís, H.d.B.S., Assmann, F., Antônio Záchia Ayub, M., et al., 2003. Purification and properties of a transglutaminase produced by a *Bacillus circulans* strain isolated from the Amazon environment. Biotechnol. Appl. Biochem. 37 (3), 295–299. https://doi.org/10.1042/ba20020110.

Luisa, A., Gaspar, C., de Goes-Favoni, S., 2015. Action of microbial transglutaminase (MTGase) in the modification of food proteins: A review. Food Chem. 171, 315–322. https://doi.org/10.1016/j.foodchem.2014.09.019.

Ma, Y., Yang, H., Chen, X., Sun, B., Du, G., Zhou, Z., Song, J., Fan, Y., Shen, W., 2015. Significantly improving the yield of recombinant proteins in *Bacillus subtilis* by a novel powerful mutagenesis tool (ARTP): Alkaline α-amylase as a case study. Protein Expr. Purif. 114, 82–88. https://doi.org/10.1016/j.pep.2015.06.016.

Monroe, A., Setlow, P., 2006. Localization of the transglutaminase cross-linking sites in the *Bacillus subtilis* spore coat protein GerQ. J. Bacteriol. 188 (21), 7609–7616. https://doi.org/10.1128/jb.01116-06.

Nkrumah, L.J., Muhle, R.A., Moura, P.A., Ghosh, P., Hatfull, G.F., William, R.J., Fidock, D.A., 2006. Efficient site-specific integration in Plasmodium Falciparum chromosomes mediated by mycobacteriophage Bxb1 integrase. Nat. Methods. 3 (8), 615–621. https://doi.org/10.1038/nmeth904.

Noda, S., Miyazaki, T., Tanaka, T., Ogino, C., Kondo, A., 2012. Production of *Streptoverticillium cinnamoneum* transglutaminase and cinnamic acid by recombinant *Streptomyces lividans* cultured on biomass-derived carbon sources. Bioresour. Technol. 104 (1), 648–651.. https://doi.org/10.1016/j.biortech.2011.10.045.

Oteng-Pabi, S.K., Keillor, J.W., 2013. Continuous enzyme-coupled assay for microbial transglutaminase. Activity Anal. 441 (2), 169–173. https://doi.org/10.1001/archinte.155.18.1973.

Phan, T.T.P., Nguyen, H.D., Schumann, W., 2012. Development of a strong intracellular expression system for *Bacillus subtilis* by optimizing promoter elements. J. Biotechnol. 157 (1), 167–172. https://doi.org/10.1016/j.jbiotec.2011.10.006.

Santhi, D., Kalaikannan, A., Malairaj, P., Arun Prabhu, S., 2017. Application of microbial transglutaminase in meat foods: A review. Crit. Rev. Food Sci. Nutr. 57 (10), 2071–2076. https://doi.org/10.1080/10408398.2014.945990.

Siegl, T., Tokovenko, B., Myronovskyi, M., 2013. Design, construction and characterisation of a synthetic promoter library for fine-tuned gene expression in actinomycetes. Metab. Eng. 19, 98–106. https://doi.org/10.1016/j.ymben.2013.07.006.

Urban, J.H., Vogel, J., 2009. A green fluorescent protein (GFP)-based plasmid system to study post-transcriptional control of gene expression in vivo. Methods Mol. Biol. 540, 301–319. https://doi.org/10.1007/978-1-59745-558-9_22.

Wang, W., Li, X., Wang, J., Xiang, S., Feng, X., Yang, K., 2013. An engineered strong promoter for *Streptomycetes*. Appl. Environ. Microbiol. 79 (14), 4484. https://doi.org/10.1128/aem.00985-13.

Yin, X., Li, Y., Zhou, J., Rao, S., Du, G., Chen, J., Liu, S., 2021. Enhanced production of transglutaminase in *Streptomyces mobaraensis* through random mutagenesis and site-directed genetic modification. J. Agric. Food Chem. 69 (10), 3144–3153. https://doi.org/10.1021/acs.jafc.1c00645.

Yokoyama, K., Nio, N., Kikuchi, Y., 2004. Properties and applications of microbial transglutaminase. Appl. Microbiol. Biotechnol. 64 (4), 447–454. https://doi.org/10.1007/s00253-003-1539-5.

Zhang, L., Ou, X., Zhao, G., Ding, X., 2008. Highly efficient in vitro site-specific recombination system based on *Streptomyces* Phage ΦBT1 integrase. J. Bacteriol. 190 (19), 6392–6397. https://doi.org/10.1128/jb.00777-08.

Zhang, L., Wang, L., Wang, J., Ou, X., Zhao, G., Ding, X., 2010. DNA cleavage is independent of synapsis during Streptomyces Phage ΦBT1 integrase-mediated site-specific recombination. J. Mol. Cell Biol. 2 (5), 264–275. https://doi.org/10.1093/jmcb/mjq025.

Zhang, L., Zhang, L., Yi, H., Du, M., Zhang, Y., Han, X., Feng, Z., Li, J., Jiao, Y., Zhang, Y., Guo, C., 2012. Enhancement of transglutaminase production in *Streptomyces mobaraensis* DSM 40587 by non-nutritional stress conditions: Effects of heat shock, alcohols, and salt treatments(Article). Kor. J. Chem. Eng. 29 (7), 913–917. https://doi.org/10.1007/s11814-011-0274-3.

Zheng, M., Du, G., Jian, C., 2002. pH control strategy of batch microbial transglutaminase production with *Streptoverticillium mobaraense*. Enzyme Microb. 31 (4), 477–481.. https://doi.org/10.1016/s0141-0229(02)00127-8.

Zhengyao, X., Nicholas, C.O.L., Felix, D.-C., Sunir, M., Margaret, C.M.S., William, R.A.B., 2008. Site-specific recombination in Schizosaccharomyces pombe and systematic assembly of a 400kb transgene array in mammalian cells using the integrase of *Streptomyces* phage phiBT1. Nucleic Acids Res 36 (1), e9. https://doi.org/10.1093/nar/gkm1123.

Zhou, C., Ye, B., Cheng, S., Zhao, L., Liu, Y., Jiang, J., Yan, X., 2019. Promoter engineering enables overproduction of foreign proteins from a single copy expression cassette in *Bacillus subtilis*. Microb. Cell Factories 18 (1), 111. https://doi.org/10.1186/s12934-019-1159-0.